Urban stressors impact lipid profiles in freshwater periphytic communities

Nicolas Mazzella, Romain Vrba, Aurélie Moreira, Nicolas Creusot, Mélissa Eon, Débora Millan-Navarro, Isabelle Lavoie, Soizic Morin

Urban stressors impact lipid profiles in freshwater periphytic communities

Nicolas MAZZELLA[1*], Romain VRBA[1,2], Aurélie MOREIRA[1], Nicolas CREUSOT[1], Mélissa EON[1], Débora MILLAN-NAVARRO[1], Isabelle LAVOIE[2], Soizic MORIN[1]

[1] INRAE, UR EABX, 50 avenue de Verdun, 33612 Cestas cedex, France

[2] INRS-ETE, 490 rue de la Couronne, Québec, QC G1K 9A9, Canada

*Corresponding author at: INRAE, UR EABX, 50 avenue de Verdun, 33612 Cestas cedex, France.

Abstract

The composition of lipids in algae are significantly influenced by environmental factors, including light intensity. Exposure to organic and inorganic contaminants can also disrupt the synthesis of fatty acids, changing the lipid composition of microalgae in periphytic communities. In this study, we looked at how a biocide such as dodecylbenzyldimethylammonium chloride (BAC 12) and two photoperiod durations can affect a biofilm's polar lipidome in a microcosm experiment. The heterotrophic compartment appeared to be raised by exposure to BAC 12 at the expense of phototrophic organisms. Additionally, the overall decline in polyinsaturated fatty acids indicated that the biofilm's phototrophic organisms were all severely impacted. However, it may be difficult to differentiate the effects of contamination from those of light, since there was no observable effect of photoperiods on the conventional fatty acid determination. The molecular species composition of both glycolipids and phospholipids was investigated in additional multivariate analyses. It was suggested that some molecular species may serve as more specific markers of light duration at the biofilm scale. Lastly, we recommend applying a similar lipidomic approach with monospecific cultures of microalgal strains in future research to support these findings, as the methodology used in this study would be applicable to other biofilm-derived microorganisms.

Keywords

Artificial light at night, dodecylbenzyldimethylammonium chloride, biofilm, microalgae, lipidomics, fatty acids.

1. Introduction

Freshwater biofilms are composed of a large variety of microorganisms, covering all kingdoms of life (bacteria, archaea, fungi, plantae, protista and animalia). Lipids can be considered as markers of the structure of a community of microorganisms. Fatty acids in autotrophic organisms, such as diatoms, green algae, cyanobacteria, and fungi, have distinct lipid profiles. Diatoms primarily consist of 14-, 16-, and 20-carbon saturated and unsaturated fatty acids (FA), while they produce minor or negligible 18-carbon FAs (Opute 1974). Chlorophyceae and cyanophyceae produce more octadecadienoic and octadecatrienoic fatty acids, while green algae produce hexadecatrienoic and hexadecatetraenoic acids more significantly (Zäuner et al. 2012). Thylakoid membranes in algae mainly consist of glycolipids, while phospholipids like phosphatidylethanolamine (PE), phosphatidylcholine (PC) and phosphatidylglycerol (PG) are less specific due to their presence in both microalgae and prokaryotic cells (Zulu et al. 2018, Li-Beisson et al. 2019). Algal lipid content is also strongly influenced by environmental factors. For instance, at low temperatures, the degree of unsaturation increases to maintain membrane fluidity and integrity, leading to an increase in polyinsaturated fatty-acids (PUFA) compared to saturated fatty-acids (SFA) and monosaturated fatty-acids (MUFA) (Fuschino et al. 2011). Light conditions are also known to affect lipid composition in algae. As lipids are important components of thylakoid membranes, they are involved in the regulation of photosynthetic capacity (Wacker et al. 2015). Lastly, exposure to organic and inorganic contaminants can likewise interfere with fatty acid synthesis, leading to a change in algae and biofilm lipid content (Robert et al. 2007, Filimonova et al. 2016, Fadhlaoui et al. 2020). Recent works have focused on fatty acids as algal biomarkers of environmental stress because their composition is very sensitive to stressors and environmental modifications (Arts et al. 2001, Demailly et al. 2019). However, the combined effects of

stressors in an urban environment and the subsequent reactions of microorganisms within biofilms remain poorly understood. An earlier research aimed at determining the individual and combined effects of urban stressors, namely dodecylbenzyldimethylammonium chloride (BAC 12) contaminant and Artificial Light at Night (ALAN)on autotrophic organisms in the biofilm (Vrba et al. 2023). This previous work revealed the predominant effects of the biocidal activity on autotrophic organisms in the environment, both at the scale of algal group (i.e., green algae, diatoms and cyanobacteria) and at the level of photosynthetic response. The evolution of major lipid classes, including phospholipids such as PE, PC and PG, glycolipids such as monogalactosyldiacylglycerol (MGDG), digalactosyldiacylglycerol (DGDG) and sulfoquinovosyldiacylglycerol (SQDG) was also determined. These previous results are complemented here by the determination of the molecular species composition within PE, PC, PG, MGDG and DGDG classes. Identification and quantification of the molecular species also allowed estimation of the major fatty acid fractions. More precisely, the following study will (i) address the effects of BAC 12 on the fatty acid composition of polar lipids through the study of molecular species, and (ii) discuss the possible effect of light (i.e., alternating or continuous photoperiod) that seemed difficult to uncouple from the strong and overlapping effect of the biocide.

2. Experimental section

2.1. Chemicals and reagents

The following polar lipid standards were purchased from Avanti Polar Lipids: 1-palmitoyl-2-oleoyl-glycero-3-phosphocholine or PC (16:0/18:1) (850457), 1-palmitoyl-2-oleoyl-sn-glycero-3-phosphoethanolamine or PE (16:0/18:1) (850757), 1-palmitoyl-2-oleoyl-sn-glycero-3-phospho-(1'-rac-glycerol) or PG (16:0/18:1) (840457), 1,2-diheptadecanoyl-sn-glycero-3-phosphocholine or PC (17:0/17:0) (850360), 1,2-diheptadecanoyl-sn-glycero-3-phosphoethanolamine or PE (17:0/17:0) (830756), 1,2-dipentadecanoyl-sn-glycero-3-phosphoethanolamine or PE (15:0/15:0) (850704), and 1,2-diheptadecanoyl-sn-glycero-3-phospho-(1'-rac-glycerol) or PG (17:0/17:0) (830456), L-α-phosphatidylserine (Soy, 99%) (sodium salt) (870336) for the phospholipid standards, and monogalactosyldiacylglycerol (840523), digalactosyldiacylglycerol (840524) and sulfoquinovosyldiacylglycerol (840525) from plant extracts as glycolipid standards. Ammonium acetate (LiChropur) were provided by Sigma-Aldrich. Palmitic acid (76119), oleic acid (O1008), heptadecanoic acid (H3500) and eicosapentanoic acid (44864) analytical standard grades (purity≥98 %) were purchased from Sigma-Aldrich. Acetonitrile, methanol (MeOH) tert-Butyl methyl ether (MTBE) and isopropanol HPLC grades were purchased from Biosolve Chimie, France. Ultrapure water (UPW) was obtained from Direct-Q® Water Purification System (Merck Millipore). Dodecylbenzyldimethylammonium chloride (BAC 12, purity≥99 %) and Benzyl-2,3,4,5,6-d_5-dimethyl-n-dodecylammonium chloride (purity>98 %) were obtained from Sigma-Aldrich and Cluzeau (France), respectively.

2.2. Experimental design

Glass slides (individual surface area: 150 cm^2) were placed in a small hypereutrophic pond in Cestas (Bordeaux, France)(Chaumet et al. 2019) for colonization by microbial biofilms.

After five months, colonized substrates were removed from the natural environment and were randomly placed in experimental channels (on day 0 = T0) under laboratory conditions as described in Vrba et al. (2023). Briefly, four experimental conditions were set up, each in pseudo-triplicates (i.e., separate 10-L channels fed by a common 10-L tank). The tanks and channels were filled with filtered (20 µm) pond water, at a room temperature of 20.5 ± 0.1°C and water temperature of 18.7 ± 0.2°C. The four conditions were as follow: two treatments under uncontaminated conditions (controls, CTRL) and two treatments exposed to 30 mg L^{-1} of BAC 12 (BAC). All channels were exposed either to normal light (NL) corresponding to a 14h day/10h night photoperiod (20 µmol m^{-2} s^{-1}) or to continuous light (CL). Treatments will be referred as CTRL-NL, CTRL-CL, BAC-NL and BAC-CL. On day 0, biofilms were collected to assess their initial lipid composition, prior to exposure to either BAC or CL. On day 10 (T10), biofilms were collected to analyse qualitative and quantitative changes in lipid profiles. Biofilms were immediately quenched in liquid nitrogen, and then collected by scraping the glass slides with a razor blade. The samples were freeze-dried (Benchtop Ro 8LZL BTF) and kept at -80°C until the extraction step.

2.3. Nutrient and BAC12 dosing in exposure water

Nutrients and mineral salts were monitored and analyzed using a Metrohm 881 Compact Ionic Chromatograph pro (Metrohm). Anion analysis (PO_4^-, NO_3^-, NO_2^-, Cl^- and SO_4^{2-}) was performed using a Supp 4/5 Guard/4.0 precolumn followed by a Metrosep A Supp5 – 250/4.0 column. The mobile phase was a mixture of a solution of 3.2 mmol L^{-1} Na_2CO_3 and a solution of 1 mmol L^{-1} $NaHCO_3$. Cation analysis (Na^+, K^+, Ca^{2+}, Mg^{2+} and NH^{4+}) was performed using a C4 Guard/4.0 precolumn followed by a Metrosep C6 - 250/4.0 column). The eluent used was a mixture of 2.5 mmol L^{-1} HNO_3 and a solution of 1.7 mmol L^{-1} 10,12-Pentacosadynoic acid (PCDA). Calibration ranges were from 20 to 1000 µg.L^{-1}. BAC 12 concentrations in the water were monitored at the beginning (T0) and the end of experiment (T10). Three samples of 20

mL were collected from each channel and stored at -20°C together with the stock solution until analysis. The samples were analyzed using an Ultimate 3000 HPLC coupled with an API 2000 triple quadrupole mass spectrometer. A Gemini® NX-C18 column (Phenomenex) was used as a stationary phase. The mobile phase was 90:10 (5 mM ammonium acetate:acetonitrile, v/v). The chromatographic seperation was done in isocratic mode with a flow rate of 0.6 mL min^{-1}. The injection volume was set at 20 µL. An internal standard of benzyl-2,3,4,5,6-d_5-dimethyl-n-dodecylammonium chloride was used, and its concentration in sample vials was typically 100 ng mL^{-1}. Samples were diluted and the calibration range was from 1 to 200 µg L^{-1}. Quality controls were regularly injected at concentrations of 5 and 25 µg L^{-1}, as well as analytical blanks. Concentration values for either BAC 12 (Table A 1) or nutrients are available in Vrba et al. (2023).

2.4. Lipid extraction

The biofilm samples (10-20 mg of dry mass) were weighed using a Mettler Toledo NS204S precision balance and placed in 2 mL microtubes with 150 mg of microbeads. The biphasic extraction procedure involved addition of 1 mL of a MTBE:MeOH (3:1, v/v) mixture and 650 µL of a UPW:MeOH (3:1, v/v) mixture. Prior to extraction, 50 µL of a PE (15:0/15:0) solution containing 100 ng $µL^{-1}$ was added as a surrogate. Samples containing microbeads were mechanically homogenized and extracted (3 cycles of 15 s) with the solvent mixtures by using a MP Biomedicals FastPrep-24 5G. The upper lipophilic phase (MTBE) was separated from the lower hydrophilic phase (UPW and MeOH) by centrifugation at 12,000 RPM. 600 µL of the lipophilic phase was collected. A second extraction step extracted (3 cycles of 15 s) was carried out after adding 700 µL of MTBE:MeOH mixture 3:1 (v/v) and 455 µl UPW:MeOH mixture 3:1 (v/v). The supernatant (MTBE) was collected again and added to the previous one. Only organic lipophilic phases (1.1 mL) were kept for further polar lipid analysis. Extracts were stored at -80°C and solvent underwent extraction as a procedural blank to verify the absence of

contamination during extracting procedures. Further details regarding the whole extraction procedure can be found in Mazzella et al. (2023b). The samples were then diluted in appropriate solvent injection (typical volume of 1 mL) and stored at -18°C until analysis within one week.

2.5. HPLC-ESI-MS/MS analysis

Lipid extracts were also analyzed with a Dionex Ultimate 3000 HPLC (Thermo Fisher Scientific, France) coupled with an API 2000 triple quadrupole mass spectrometer (Sciex, France). Chromatographic separation of both glycolipids and phospholipids was performed on a Luna NH2 HILIC column (3 µm, 100 × 2 mm) with a Security Guard cartridge NH2 (4 × 2.0 mm). The injection volume and temperature were set to 20 µL and 40°C, respectively. The chromatographic separation and mass spectrometry conditions are described in Mazzella et al. (2023a), (2023b). Quantitation of phosphatidylcholine (PC), phosphatidylethanolamine (PE) and phosphatidylglycerol (PG) were respectively carried out with: PC (16:0/18:1), PE (16:0/18:1), PG (16:0/18:1). Quantitation of glycolipids was carried out with MGDG (16:3_18:3) (63 % of the total MGDG standard), DGDG (18:3/18:3) (22 % of the total MGDG standard), and SQDG (34:3) (78 % of the total SQDG standard). The internal standards utilized were PC (17:0/17:0) for PC phospholipids, PE (17:0/17:0) for PE phospholipids and both MGDG and DGDG glycolipids, and PG (17:0/17:0) for PG and SQDG. Concentrations for both phospholipids and glycolipids were reported in nmol mg^{-1} (dry weight), and the limits of quantification were typically between 0.02-0.05 nmol mg^{-1}, depending on analyte response.

In addition to intact lipids, free fatty acids were analyzed by RPLC-ESI-MS/MS using the same analytical equipment. However, in that case, chromatographic separation was performed on a Kinetex C8 column (2.8 µm, 100 x 2.1 mm). Heptadecanoic acid (C17:0) was used here as an internal standard. Finally, the chromatographic and acquisition parameters are given in the appendices (Table A 2 and Table A 3).

2.6. Phospholipid and glycolipid nomenclatures

Polar glycerolipids are constituted of a glycerol backbone esterified by two fatty acids on the sn-1 and sn-2 positions. The moiety linked to the sn-3 position refers to the polar head group (e.g., sn-phospho-3-glycerol for the PG, a β-D-galactosyl group for MGDG). Each polar head group defines a phospholipid or glycolipid class, and each class can be divided into several molecular species according to the fatty acyl chain composition and distribution. When the fatty acyl chain structures are resolved but the sn-1 and sn-2 positions remain unclear, then the phospholipids or glycolipids are designated PL (C:n_C:n), with C referring to the sum of the number of carbon atoms and n to the number of double bonds for each fatty acyl chain.

2.7. Conversion of phospholipids and glycolipids to fatty acid equivalents

Following the analysis of the different classes of polar lipids, and using the molecular species within each class, the different fatty acids were determined from the acyl chains previously identified. To this purpose, each mole of each molecular species was converted into its fatty acid equivalent.

Equation 1 $1\ mole\ of\ MGDG(16{:}3/18{:}3) \rightarrow 1\ mole\ of 16{:}3 + 1\ mole\ of 18{:}3$

Equation 2 $1\ mole\ of\ PG(18{:}1/18{:}1) \rightarrow 2\ moles\ of\ 18{:}1$

Equation 1 illustrates the case where the acyl chains are asymmetric (i.e. the fatty acid at *sn-1* is different from that at *sn-2*), while Equation 2 corresponds to the case where two fatty acids with both the same numbers of carbons and unsaturations are present.

2.8. Data analyses

Data were processed using R 4.2.2 software (R Core Team, 2022) as well as Excel 2016 with XLstat 2010 add-on statistical software. Each Principal Components Analysis (PCA) was performed with Pearson correlations. Non-parametric tests (Kruskal-Wallis) and multiple

comparison methods (Conover and Iman) were respectively carried out with a global p-value ≤0.05 and Bonferroni corrections. Multivariate analysis of variance (MANOVA) and subsequent analysis of variance (ANOVA) were performed with Welch test corrections.

3. Results

3.1. Fatty acids from polar lipids

Fatty acids obtained from PG, PE, PC, MGDG and DGDG, as well as free fatty acids (FFA) (Table A 4), were plotted on a Principal Component Analysis (PCA) (Figure 1 and Figure A 1). It should be noted that FFA generally represented a small proportion with 3 to 12% of the total fatty acids quantified in the various sample extracts, regardless of the condition applied (Figure A 2). Polyunsaturated fatty acids (C16:3, C18:3, C20:2, C20:3, C20:4, C20:5, C22:5 and C22:6) loaded along axis 1. These PUFAs appeared to be more abundant in the samples under CTRL conditions, both at the initial time (T0) and after 10 days of exposure. Conversely, two saturated fatty acids and monounsaturated fatty acids (16:1, 18:0 and 18:1) were most abundant after exposure to BAC12 for 10 days (Vrba et al. 2023). The second axis of the PCA only explained 15.0 % of the total inertia compared to 46.7 % for the first axis. This second axis did not allow for a clear discrimination of other factors, such as a possible effect of normal light (NL) or continuous light (CL) conditions. Another representation can be obtained with a combination of the second and the fourth axes (6.4 %), with however a consequent overlapping of the confidence intervals for T10 CTRL-NL and–CL samples (Figure A 1).

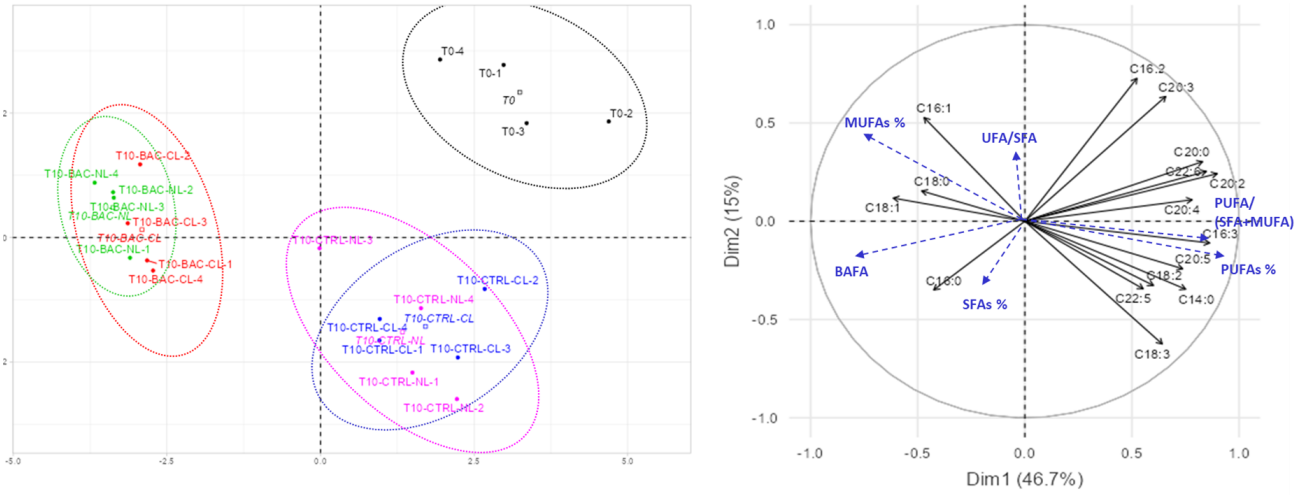

Figure 1. PCA (dimensions 1 and 2) with initial samples (T0), controls after 10 days (T10 CTRL) according to continuous (CL) or normal (NL) light, as well as samples contaminated with BAC 12, after 10 days (T10 BAC) and also with the two light conditions (CL and NL). The variables represented on the right correspond to fatty acids determined from polar lipids, as well as free fatty acids. % SFAs, MUFAs and PUFAs as well as BAFA, UFA/SFA and PUFA/(SFA+MUFA) ratios are represented as supplementary variables in blue.

The amounts of fatty acids (in nmol mg^{-1} of dry biofilm) obtained from the molecular species of the phospholipids PG, PE and PC are presented in of Figure 2 (A1, B and C). These barplots are presented only for the alternating photoperiod NL condition because the PCA previously indicated that photoperiod did not markedly contribute to biofilm fatty acid composition. The results presented in Figure 2 suggest a near disappearance of C20:5 within PG, while C16:0, C16:1 and C18:1 highly increased in the presence of BAC 12. Panel A2 presents fatty acids from PG according to the categories SFAs, MUFAs and PUFAs. For the uncontaminated controls, MUFAs seemed to be in the majority (58-63%) under normal light condition at both T0 and T10. However, MUFAs appeared to be in equivalent proportion to SFAs (39 and 37%, respectively) in the continuous light condition. PUFAs also seemed to increase in the T10-CTRL-CL, however, this remains a trend as no significant differences were found according to a non-parametric Kruskal-Wallis test. When considering either T10-BAC-NL or CL samples a drastic decrease in PUFAs, essentially in favor of MUFAs, was observed

239 in the presence of BAC 12. It should be noted that C20:5, which composed the majority of the
240 PUFAs in the CTRL samples, disappeared completely with exposure to the biocide.

241 The initial fatty acid composition (T0) from PE (Figure 2, panel B), as well as the
242 composition after 2 and 10 days of experiment without BAC12 contamination, differed from
243 that of PG where C18:2 and C18:3 were abundant and where C20:5 and C20:4 showed very
244 low concentrations. Within the same phospholipids, and as observed for PG, an increase in
245 MUFAs with 16 or 18 carbon atoms was observed, as well as the SFA C16:0. Finally, PC was
246 characterized by an equivalent distribution of C18:2, C18:3 and C20:5 within the PUFAs from
247 this class of membrane lipids, with contents essentially between 0.2 and 0.4 nmol mg^{-1} (Figure
248 2, panel C). We did not observe an increase in SFAs or MUFAs as a result of decreasing PUFAs.
249 The results rather suggest that it is the fatty acids from PC that decreased in absolute values.

250

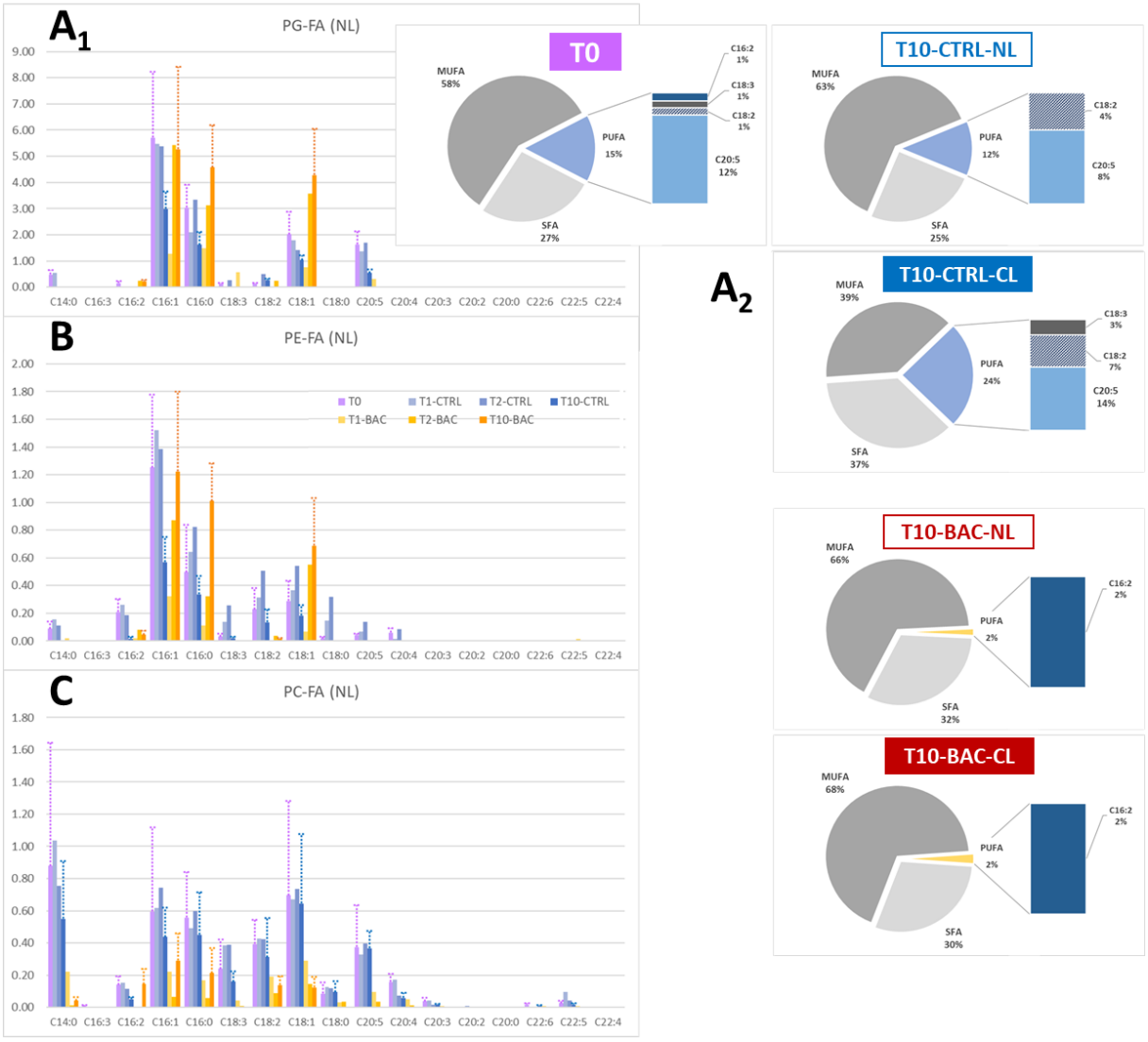

Figure 2. Evolution of fatty acids (nmol mg^{-1}) deduced from the molecular species of phospholipids (A1) PG, (B) PE and (C) PC. Different times are reported here with 1, 2 and 10 days of culture with or without BAC 12 and under normal light conditions. Part A2 on the right illustrates for PG the grouping of fatty acids (% mol) within SFA, MUFA and PUFA, and then the details for PUFAs only, for T0 and T10 samples.

Afterward, we considered the fatty acids associated with MGDG and DGDG. As explained in Mazzella et al. (2023a), the method we used did not allow for the identification of the acyl chains of SQDG, and therefore did not allow for an accurate determination of associated fatty acids. Panels A1 and B of Figure 3 shows the evolution of the content of each fatty acid within MGDG or DGDG. The most striking response was the near disappearance of all fatty acids upon exposure to BAC 12, whatever the light conditions, and this was observed

from the first day. This may result from the sharp decline in MGDG and DGDG under those same conditions, as previously observed in Vrba et al. (2023).

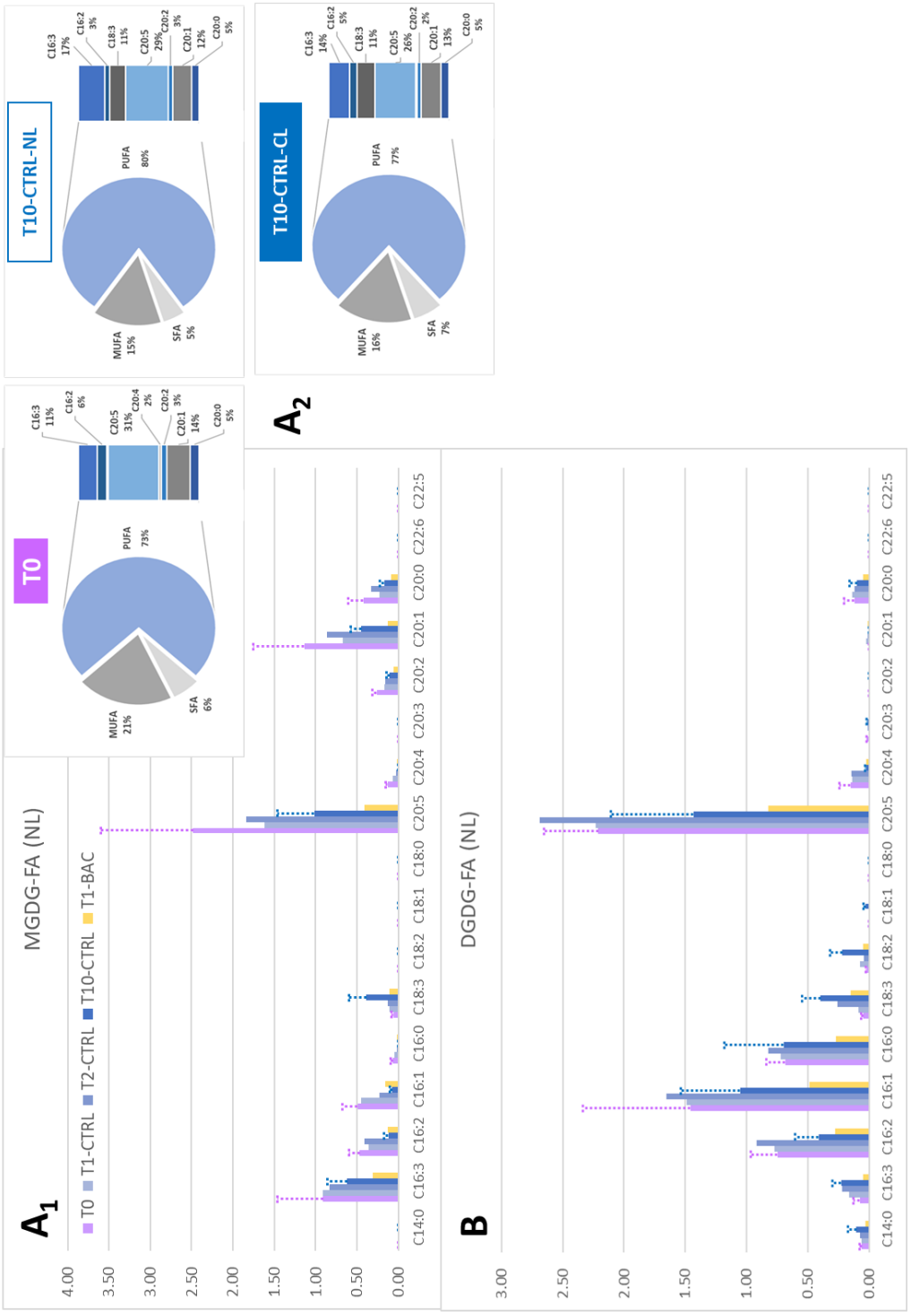

Figure 3. Evolution of fatty acid concentrations (nmol mg^{-1}) calculated from the molecular species of glycolipids (A1) MGDG, (B) DGDG. Panel A2 illustrates fatty acids (% mol) within SFA, MUFA and PUFA for MGDG as well as individual PUFAs.

In the absence of contamination, C20:5 was the most abundant fatty acid in MGDG with both photoperiods (Figure 3, panel A2), followed by C16:3, C16:2 and C16:1 and long chain fatty acids such as C20:1 and C20:0. All fatty acids decreased over time with the exception of C18:3, which became more abundant at T10. Panel A2 of Figure 3 shows a noticeable stability in SFA, MUFA and PUFA after 10 days of growth in the artificial river channels. Looking at the relative proportions of each PUFAs, we could see a clear increase in C18:3 at the final sampling time with a relative proportion of almost 11 % compared to less than 1 % at the initial time. The fatty acid composition of DGDG was quite distinct from that of MGDG, with a more abundant pool of 16-carbon fatty acids, particularly centered around C16:1. The SFA, MUFA and PUFA categories are not represented here, however they appeared rather similar with a clear majority of PUFAs, as well as an equally stable composition over time in the samples not exposed to BAC 12.

3.2. Molecular species from polar lipids

The molecular species identified within the main classes of PG, PE, PC, MGDG and DGDG are presented in Figure 4. The area of each rectangle is proportional to the relative amount in molar %. Only T0 and T10 under normal light conditions, with or without exposure to BAC 12, are shown. A very similar trend was observed under continuous light conditions and was consequently not illustrated here. At T0, PG clearly dominated with approximately 41%, then MGDG and DGDG with 20 and 17%, respectively. These polar lipids are generally associated with thylakoid membranes in plants. Together, PC and PE represented less than a quarter of the polar lipids. These compounds are more representative of cytoplasmic membranes in plants. As with the fatty acids, we observed several molecular species containing at least one PUFA on each of the two acyl chains of each glycerolipid. In the case of PG, and especially MGDG and DGDG, we observed that most fatty acids were a combination between

296 eicosapentaenoic acid (EPA or C20:5) and a SFA or a MUFA such as C16:0, C16:1, C20:0 and
297 C20:1.To a lesser extent, C20:5 appeared to be associated with C16:2 or C16:3.

298 After a 10-day exposure in the channels under normal light (T10-CTRL-NL), MGDG
299 decreased in proportion comparable to DGDG and PC. Overall, we still observed many
300 molecular species containing 1 or 2 PUFAs, but there was a slight increase in the representation
301 of combinations between 16:3, 18:2 and 18:3 compared to the initial condition (T0). With the
302 exposure to the biocide BAC 12 (T10-BAC-NL), we observed a radical change in both classes
303 (i.e. MGDG and DGDG), with the general disappearance of the two glycolipids, as well as an
304 apparent decrease in the number of compounds containing at least one PUFA. Thus, we were
305 able to discern the presence of PG (16:0_16:1), PG (16:0_18:1) or PG (16:1_18:1). The same
306 applies to PE, the second most abundant phospholipid (PG and PE representing almost 96% of
307 the initial polar lipids), with essentially mostly combinations between C16:0, C16:1 and C18:1.

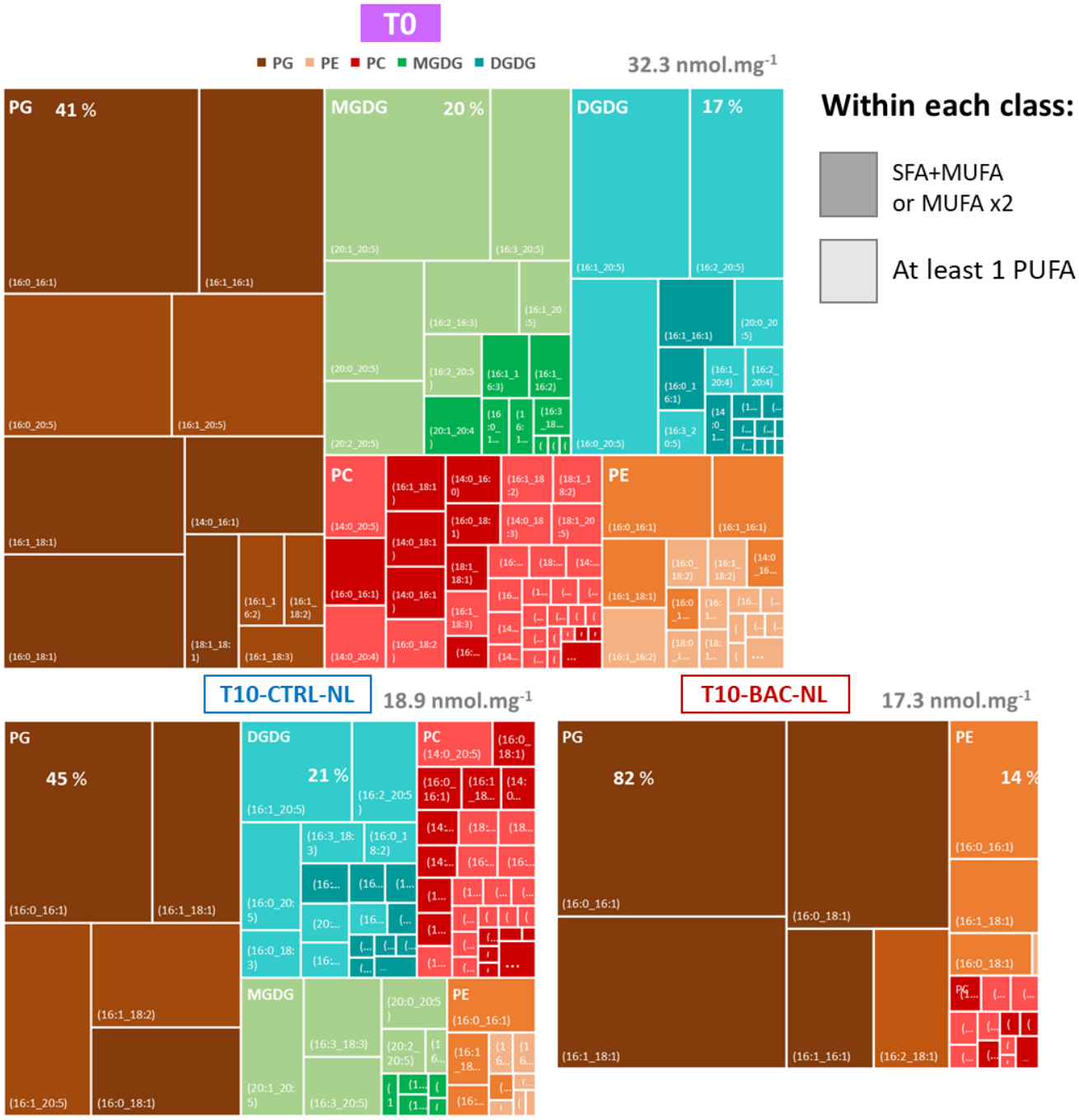

Figure 4. Tree-map of molecular species, belonging to each of the polar lipid classes, detected for samples at T0 and T10, contaminated or not with BAC, and for alternating/normal light (NL) only. The surface of each block is proportional to the amount in nmol mg^{-1}.

3.3. Covariation of polar lipid classes and fatty acid categories

A clear effect of BAC 12 on the evolution of both absolute and relative amounts of lipid content in freshwater biofilms has been shown here at the fatty acid level, as previously reported

316 at the lipid class level in Vrba et al. (2023). For each date and condition, we have plotted on
317 abscissa the ratio between the average amount of glycolipids (GL), represented here by all
318 molecular species of MGDG and DGDG, and the average amount of phospholipids (PL) such
319 as PG, PE and PC (i.e. GL/PL ratio). The ordinate is another ratio comprising all PUFAs (from
320 all the classes) over the sum of the MUFAs and SFAs determined simultaneously in the same
321 samples (i.e. (PUFA/(MUFA+SFA) ratio). In the top right-hand quadrant, for GL/PL and
322 PUFA/(MUFA+SFA) ratios between 0.5 and 1.1, we can observe all the samples over the time,
323 and whatever the photoperiod applied, corresponding to non-contaminated conditions. The
324 unique and significant effect of BAC 12 was supported with a MANOVA for the two ratios
325 (Table A 6). These are probably the highest values that the two indices can reach, indicating at
326 the same time a proportion of PUFAs between one third and one half of all fatty acids, and a
327 proportion of glycolipids between 30 and 40% of all polar lipids of both thylakoids and cell
328 membranes. On the other hand, the lower left quadrant, with proportions that are both close to
329 zero, i.e. the near disappearance of glycolipids and PUFAs, consists exclusively of samples
330 contaminated with BAC 12. It should also be noted that the samples did not appear to be
331 differentiated, whatever the light condition applied (NL or CL). These results suggested that
332 PUFAs, even when considered as a whole, are essentially associated with glycolipids in this
333 biofilm. In other words, the joint disappearance of MGDG and DGDG would lead to a
334 consequent and sharp decrease in this category of fatty acids. The results of corresponding
335 Welch's ANOVA was provided as supplementary information (Figure A 3).

336

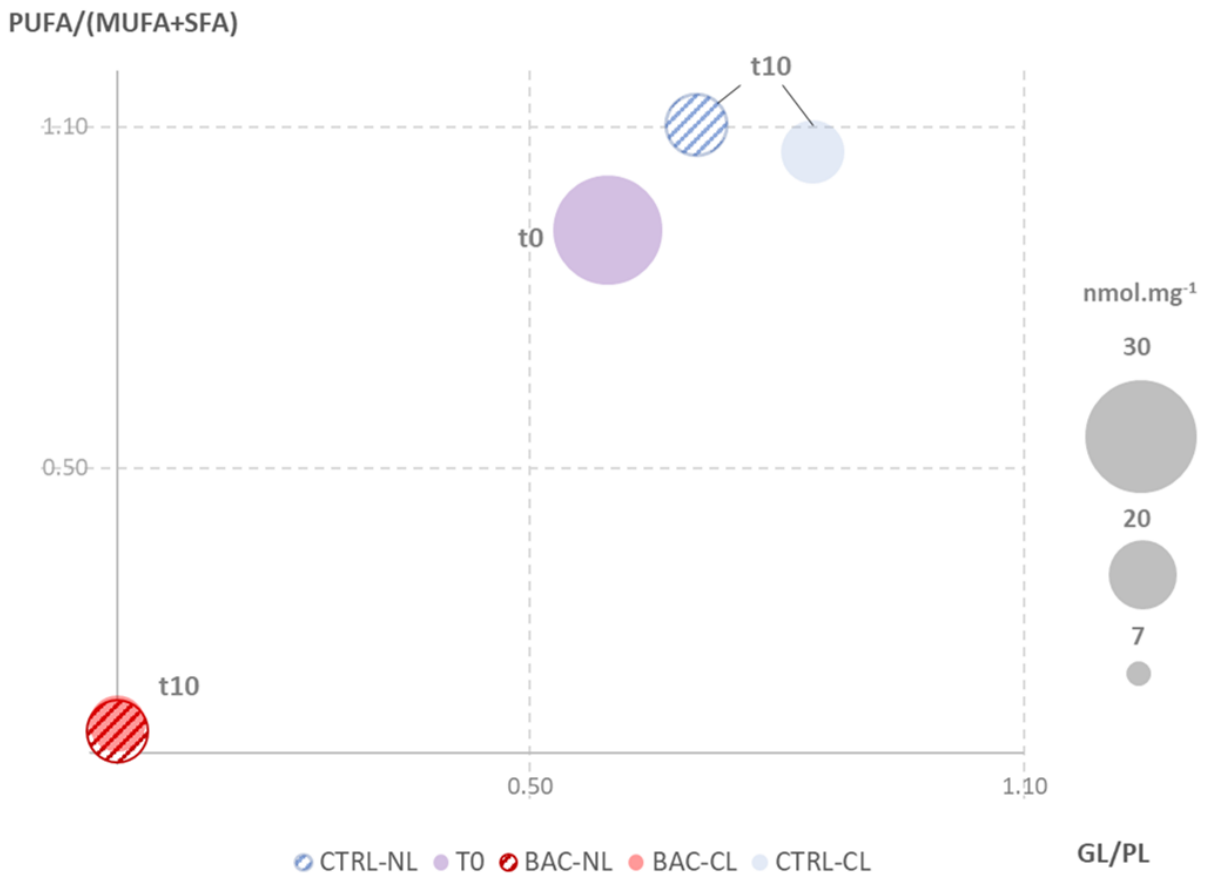

337

338 Figure 5. Two-dimension scatter plot of samples over time, contaminated or not with BAC 12,
339 and with two light conditions. The size of the circle corresponds to the mean quantity of polar
340 lipids per sample and per condition.

341

342

4. Discussion

4.1. BAC 12 effects over the time

The results presented in Figure 1, Figure 2 and Figure 3 showed that the samples contained polyunsaturated fatty acids in the absence of BAC 12, indicating that the biofilms contained photoautotrophs belonging to the bacillariophyceae, chlorophyceae and cyanophyceae groups (Vestal and White 1989, Guschina and Harwood 2009). This was also confirmed by fluorimetry and microscopy analyses (Vrba et al. 2023). Bacterial FA (BAFA index) with the sum of some SFAs and MUFAs like C15:0, C15:1, C16:0, C17:0, C17:1, C18:0 and C18:1n-7 (Napolitano 1999, Dalsgaard et al. 2003) can also be used to estimate the contribution of bacteria to the biofilm community. The projection of the BAFA index among the additional variables in the PCA (Figure 1) could indicate an increase of the heterotrophic compartment over the time, under BAC 12 exposure, at the detriment of phototrophic organisms. In Figure A 1, axis 4 seems to allow for the separation between the continuous and alternating light conditions only in the T10-CTRL samples. This subtle distinction seems to be attributed to C16:0 and C18:3, which contributed more markedly to the CL condition, whereas C18:1 and C18:2 contributed more markedly to the NL condition. However, certain of these fatty acids (i.e., C18:2 and C18:3) were also potentially impacted by the presence or absence of BAC12 and, therefore, it becomes difficult to clearly disentangle the two factors solely based on the fatty acid composition of the polar lipids. The disappearance of certain classes of lipids (e.g., MGDG and DGDG) during exposure to BAC 12 has already been observed in the previous work conducted by Vrba et al. (2023). The overall decrease in PUFAs observed here on the same samples, also suggests a drastic decrease of all phototrophic organisms within the biofilm. It should be noted that other contaminants such as S-metolachlor, diuron, nickel or copper also caused a significant decrease in PUFAs in microalgal cultures or biofilms compared

368 to other fatty acid categories (Filimonova et al. 2016, Demailly et al. 2019, Fadhlaoui et al.
369 2020).

370 An additional data treatment consisted in a PCA using the molecular species
371 composition of MGDG, DGDG, PG, PE and PC, in order to better distinguish the likely effects
372 of BAC12 and light condition at the algal group level. The variables described in the F1-F2
373 plane of the PCA (Figure 6) were sorted according to their decreasing contribution to these two
374 axes, including only those with $\cos^2 > 0.7$ (Table 1). A clustering of these filtered variables was
375 then performed using a k-means classification (Figure A 4), resulting into three "variable
376 clusters", namely F2a, F1,2a and F1,2b. A fourth cluster has been identified, but when projected
377 onto the variable plot (Figure 6), it did not appear to provide any sample- or condition-specific
378 information. Additionally, we attempted to reassign molecular species to different autotrophic
379 groups based on information from the literature (Opute 1974, Dunstan et al. 1993, Bergé et al.
380 1995, Lang et al. 2011, Coniglio et al. 2021, Mazzella et al. 2023a). For example, molecular
381 species containing C14:0, C20:5 or C22:6 were preferentially related to diatoms. In contrast,
382 compounds with C18:2 or C18:3 associated with another 16- or 18-C SFA or MUFA were
383 preferentially linked to contributions from green algae or cyanobacteria. Finally, when the
384 molecular species appeared to be non-specific to a particular microbial groups (e.g. associations
385 primarily among C16:0, C16:1 and C18:1), we indicated that it was an undetermined origin.
386 Actually, it is possible to find such molecular species in all eukaryotic algae (Guschina and
387 Harwood 2006), in fungi (Bhatia et al. 1972) as well as in prokaryotic organisms (Zelles 1997,
388 Doumenq et al. 1999, Mazzella et al. 2005, Mazzella et al. 2007, Sohlenkamp and Geiger 2015).

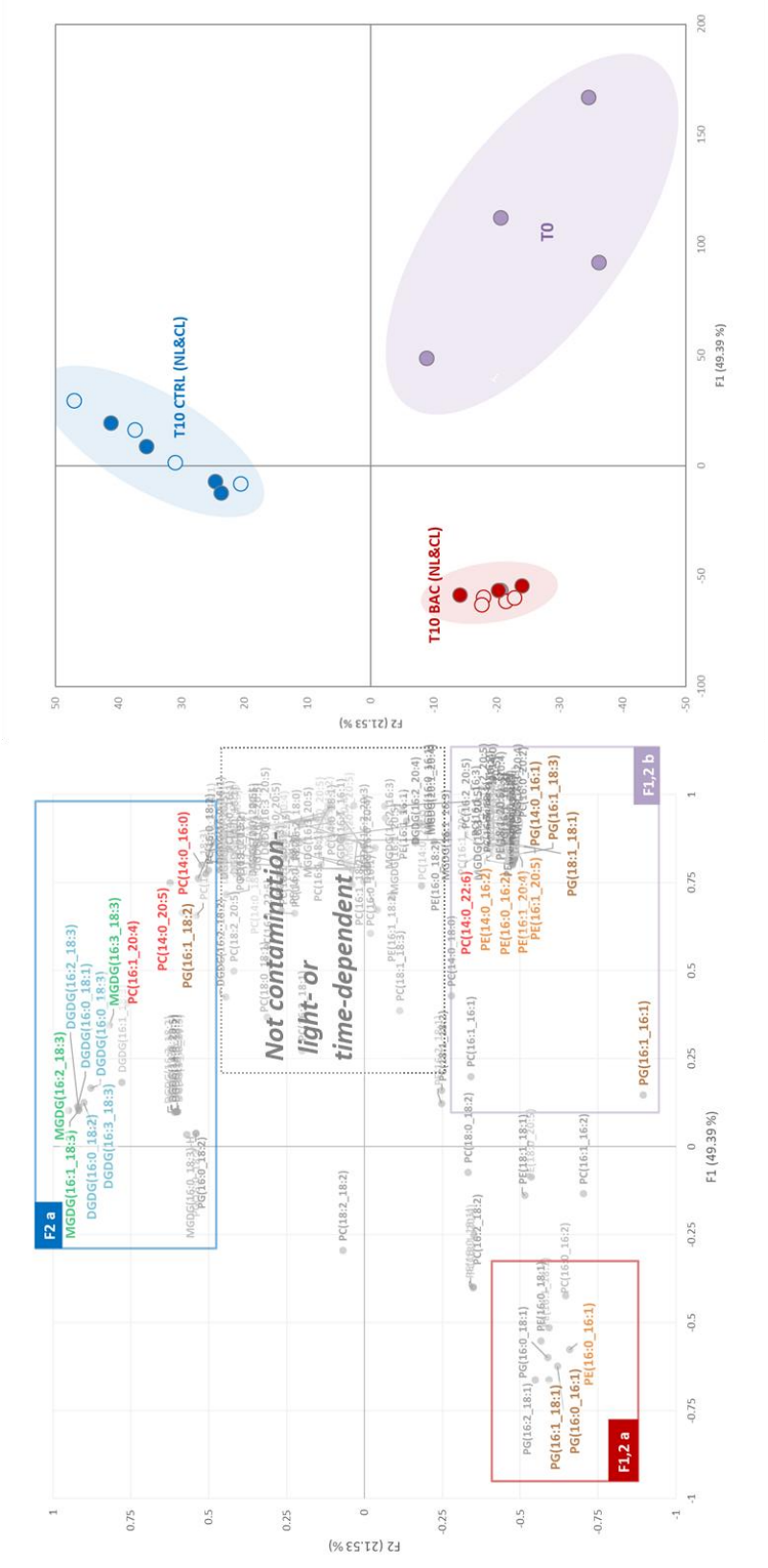

389

390 Figure 6. F1- F2 plan of the PCA with the initial samples (T0), the controls after 10 days (T10
391 CTRL) under continuous (CL) or alternating (NL) light, as well as the samples contaminated
392 with BAC 12 after 10 days (T10 BAC) under the two light conditions (CL and NL). The
393 variables shown on the left correspond to the set of molecular species associated with polar
394 lipids.

Table 1. Molecular species filtered from the PCA results, considering the 20% of variables contributing the most to the F1 and F2 axes, as well as with a $cos^2 > 0.7$ for the sum F1+F2. Three clusters of variables (F2a, F1,2a and b) were defined, and likely attributions of the variables was proposed according to the fatty acid composition highlighted within the selected molecular species.

Molecular species	Top 20 % contributions axis F1+F2	$Cos^2 > 0.7$ axis F1+F2	Correlation significance[1]	Variable clusters	Likely algal attributions
DGDG(16:0_18:1)	3.010	0.863	***	F2 a	N.D.
DGDG(16:0_18:2)	2.981	0.854	***	F2 a	Chloro+Cyano
DGDG(16:0_18:3)	2.766	0.802	***	F2 a	Chloro+Cyano
DGDG(16:2_18:3)	2.980	0.853	***	F2 a	Chloro+Cyano
DGDG(16:3_18:3)	2.888	0.830	***	F2 a	Chloro+Cyano
MGDG(16:1_18:3)	2.980	0.853	***	F2 a	Chloro+Cyano
MGDG(16:2_18:3)	3.203	0.916	***	F2 a	Chloro+Cyano
MGDG(16:3_18:3)	2.547	0.791	***	F2 a	Chloro+Cyano
PC(14:0_16:0)	1.940	0.911	***	F2 a	Diatoms
PC(14:0_20:5)	2.235	0.950	***	F2 a	Diatoms
PC(16:1_20:4)	2.300	0.747	*	F2 a	Diatoms
PG(16:1_18:2)	1.888	0.785	**	F2 a	Chloro+Cyano
PE(16:0_16:1)	2.038	0.768	**	F1,2 a	N.D.
PG(16:0_16:1)	1.945	0.773	**	F1,2 a	N.D.
PG(16:1_18:1)	1.902	0.789	***	F1,2 a	N.D.
PC(14:0_22:6)	1.962	0.990	*	F1,2 b	Diatoms
PE(16:0_16:2)	1.971	0.993	***	F1,2 b	Chloro+Cyano
PE(16:1_20:4)	1.962	0.989	***	F1,2 b	Chloro+Cyano
PE(16:1_20:5)	1.953	0.967	***	F1,2 b	Diatoms
PG(14:0_16:1)	1.949	0.977	***	F1,2 b	Diatoms
PG(16:1_16:1)	2.846	0.821	***	F1,2 b	N.D.
PE(14:0_16:2)	1.980	0.988	***	F1,2 b	Chloro+Cyano
PG(16:1_18:3)	1.882	0.924	*	F1,2 b	Chloro+Cyano
PG(18:1_18:1)	1.963	0.974	***	F1,2 b	N.D.

[1] *p-value <0.05 (*), <0.01 (**), <0.001 (***) for correlations with F1 or F2*

Cluster F2a was associated with the T10 CTRL samples, regardless of the photoperiod condition, while cluster F1,2b was associated with the initial samples at T0. Cluster F1,2b seemed to be more strongly related to the exposure to BAC 12 during the entire 10 days of exposure. This result suggests that the presence of such a biocide exerts a selective pressure on the different microorganisms constituting the biofilm, with a progressive elimination of microalgae in favor of fungi or prokaryotes (Sakagami et al. 1989). These findings observed at the molecular species level thus confirm the conclusions drawn from the taxonomic observations formulated by Vrba et al. (2023). We may thus propose some potential biomarkers by grouping increasing response of PC molecular species such as (14:0_16:0), (14:0_20:5) and (16:1_20:4), assumed to be here diatom-originating, in samples not contaminated with BAC 12 (Figure 7). However, it would be interesting to investigate further the degree of specificity of

this type of response to a specific contaminant in benthic microalgae at the level of lipid molecular species, especially with axenic culture conditions.

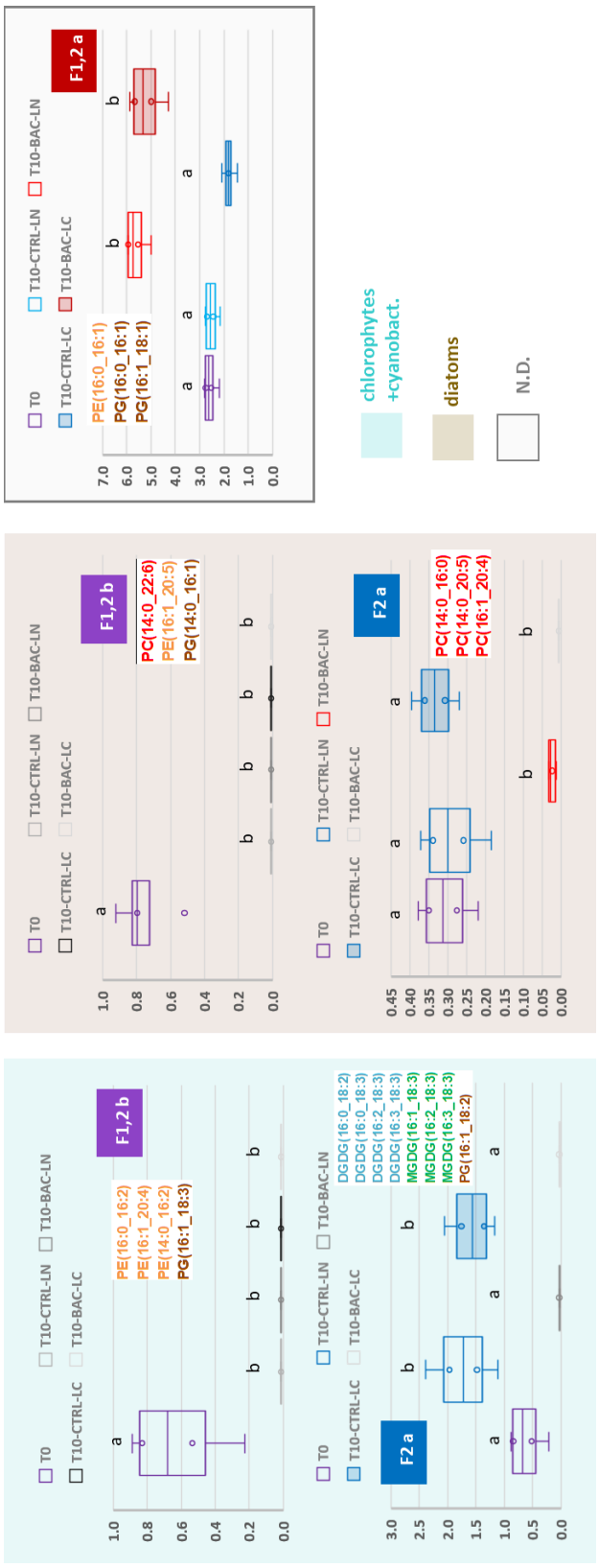

Figure 7. Variation of selected molecular species clusters (nmol mg^{-1}) for each group of variables (F2 a, F1,2 a and b) as a function of time (T0 or T10), BAC 12 (CTRL or BAC) as well as the continuous or normal light conditions (CL or NL). The distinction was also made based on the likely origin of the molecular species, according known and representative fatty acids of certain autotroph groups.

4.2. Continuous versus alternated photoperiods

No significant effect of the light condition (i.e., NL or CL) was observed on fatty acids derived from polar lipids. Vrba et al., 2023 came to the same conclusion based on analyses of the same samples at the level of lipid classes. This results in a difficulty to dissociate a possible effect of light condition from that of the contaminant. Because this study address also the molecular species, it is possible to keep information associated with the various fatty acids that can be attributed to specific microorganism groups from the biofilm. Actually, it become possible to attribute them either a phototrophic origin (i.e. PUFAs acyl chains of the MGDGs and DGDGs) or a heterotrophic origin (e.g. C16:0, C16:1 or C18:1 acyl chains of the PGs or PEs). Furthermore, in relation to light conditions, MGDG is thought to play an important role in the operation of the xanthophyll cycle in the thylakoid membranes of algae, including diatoms (Goss and Jakob 2010). MGDG is also present in cyanobacteria, the ancestors of chloroplasts in other photosynthetic organisms, even if the prokaryotic thylakoids do not operate a xanthophyll cycle, as found in algae. In addition, the development of thylakoid membrane networks, and therefore an effective photosynthesis, depends on a coordinated biosynthesis of thylakoid lipids with chlorophylls and photosynthetic proteins during chloroplast biogenesis, and both MGDG and DGDG plays a key-role during these processes (Wada and Murata 1998).

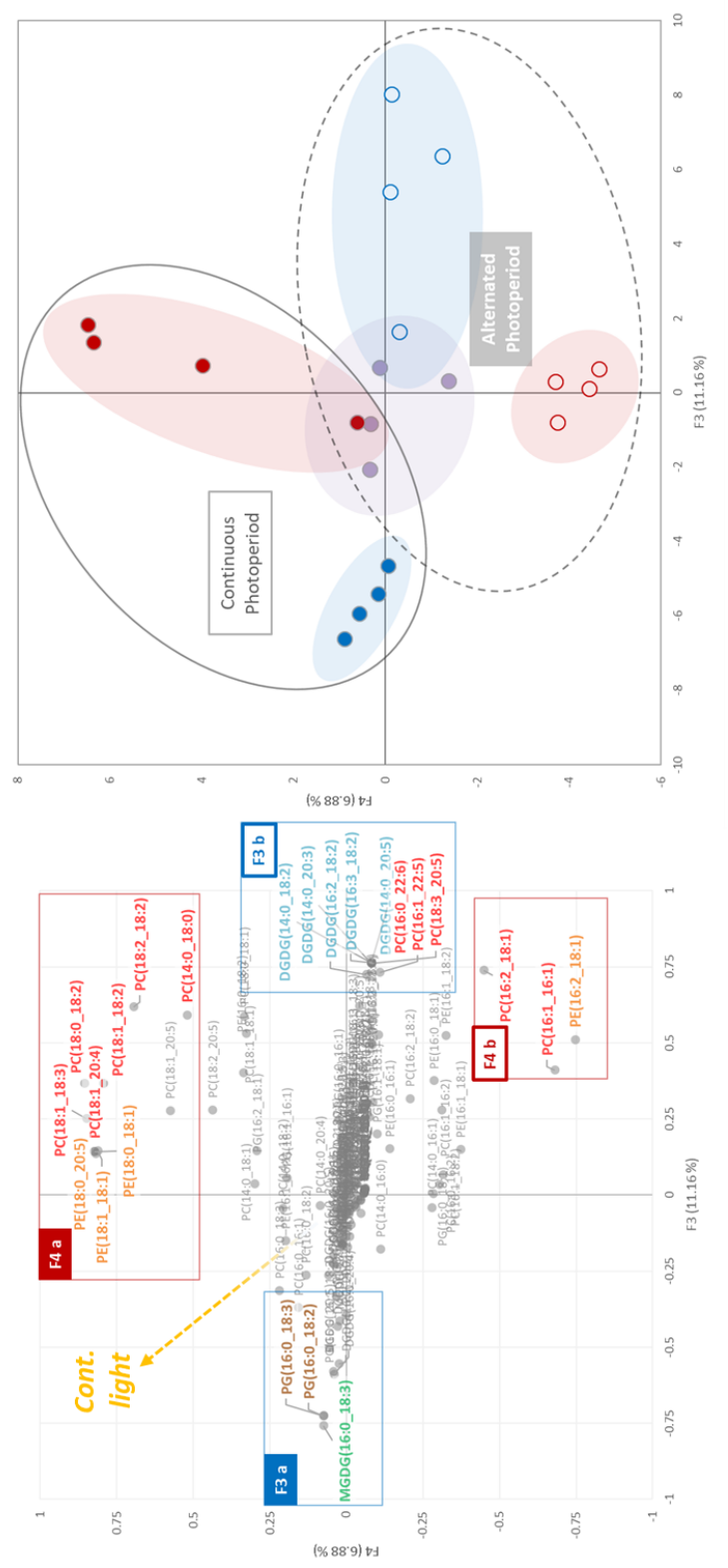

Figure 8 F3- F4 planes of the PCA with the initial samples (T0), the controls after 10 days (T10 CTRL) under continuous (CL) or normal (NL) light, as well as the samples contaminated with BAC 12 after 10 days (T10 BAC) under the two light conditions (CL and NL). The variables shown on the left correspond to the set of molecular species associated with polar lipids. The continuous light vector is a supplementary variable.

Focusing on F3 and F4 axes of the PCA, a more specific discrimination related to the photoperiod was observed, as shown by the projection of this additional variable in the left part the graph (Figure 8). We then filtered the variables best represented in this F3-F4 plane of the PCA (Table 2) and defined four clusters (Figure A 4), as well as the probable assignment to specific algal groups. It is interesting to note that this analysis allowed the distinction between the samples that have undergone a continuous photoperiod from those that have been treated with an alternating photoperiod, as they appeared to be separated according to the first bisector associated with axes 3 and 4. Thus, the presence or absence of BAC 12 under the NL condition (i.e. alternating photoperiod) was distinguished by the two clusters F3b and F4b. On the other hand, the presence or absence of BAC 12 resulted in two other clusters, F3a and F4a, which were more indicative of the CL condition. Moreover, according to this clustering of variables, it seems that the continuous photoperiod may induce a relative increase in molecular species associated with green algae and cyanobacteria to the detriment of those originating from diatoms. In other words, the change in lipid composition revealed by molecular species analysis indicated that the CL condition would promote the growth of certain photoautotroph groups over time, regardless of the contamination pressure. Wang and Jia (2020) studied the photoprotective mechanisms of *Nannochloropsis oceanica* in response to light, mainly from the point of view of lipid and fatty acid classes, in parallel with the study of pigment composition. These authors showed that at higher intensities, there was a fairly marked decrease in MGDG and DGDG, but also in phospholipids. They also observed a decrease in most of the fatty acids associated with polar lipids, but this did not appear to be specific to certain categories such as PUFAs. The notable difference with our study is that the authors conducted their experiment on an algae culture while we studied the response of biofilms. In addition, they increased light intensities from 50 to 500 µmol m^{-2} s^{-1} (20 µmol m^{-2} s^{-1} for our study) with a continuous photoperiod only.

Table 2. Molecular species filtered from PCA results considering 30% of variables contributing the most to the plane described by F3 and F4, as well as with a $cos^2 > 0.5$ for the sum F3+F4. Four clusters of variables (F3a and b, F4a and b) were defined, and likely attributions of the variables was proposed according to the fatty acid composition highlighted within the selected molecular species.

Molecular species	Top 30 % contributions axis F3+F4	$Cos^2 > 0.5$ axis F3+F4	Correlation significance[1]	Variable clusters	Likely algal attributions
PG(16:0_18:2)	3.648	0.534	***	F3 a	Chloro+Cyano
PG(16:0_18:3)	3.648	0.534	***	F3 a	Chloro+Cyano
MGDG(16:0_18:3)	3.979	0.582	***	F3 a	Chloro+Cyano
PC(14:0_18:0)	5.355	0.619	**	F4 a	Diatoms
PC(18:0_18:2)	8.991	0.868	***	F4 a	Chloro+Cyano
PC(18:1_18:2)	7.840	0.763	***	F4 a	Chloro+Cyano
PC(18:1_18:3)	8.371	0.784	***	F4 a	Chloro+Cyano
PC(18:1_20:4)	7.614	0.699	***	F4 a	Diatoms
PC(18:2_18:2)	7.909	0.864	**	F4 a	Chloro+Cyano
PE(18:0_18:1)	7.606	0.698	**	F4 a	N.D.
PE(18:0_20:5)	7.505	0.689	***	F4 a	Diatoms
PE(18:1_18:1)	7.415	0.681	***	F4 a	N.D.
PC(16:0_22:6)	3.992	0.584	***	F3 b	Diatoms
PC(16:1_22:5)	3.751	0.545	***	F3 b	Diatoms
PC(18:3_20:5)	3.991	0.584	**	F3 b	Diatoms
DGDG(14:0_20:5)	4.017	0.587	***	F3 b	Diatoms
DGDG(14:0_18:2)	4.018	0.588	***	F3 b	Chloro+Cyano
DGDG(14:0_20:3)	4.011	0.587	*	F3 b	Diatoms
DGDG(16:2_18:2)	3.596	0.527	***	F3 b	Chloro+Cyano
DGDG(16:3_18:2)	4.026	0.589	***	F3 b	Chloro+Cyano
PC(16:1_16:1)	6.217	0.629	**	F4 b	N.D.
PC(16:2_18:1)	5.906	0.745	*	F4 b	Chloro+Cyano
PE(16:2_18:1)	7.895	0.816	***	F4 b	Chloro+Cyano

[1] *p-value <0.05 (*), <0.01 (**), <0.001 (***) for correlations with F3 or F4*

The lipid content of algae is also significantly affected by light cycles. For example, Brown et al. (1996) studied the effects of different light regimes on the lipids of the diatom *Thalassiosira pseudonana* where 100, 50 and 100 µmol m^{-2} s^{-1} under respective 12:12, 24:0 and 24:0 h light/dark cycles were used. Cells grown at the high light intensity and 12:12 photoperiod exhibited higher concentrations of PUFAs and lower concentrations of both SFAs and MUFAs. Although it is very likely that the duration of the photoperiod also affected the autotrophs found in our biofilms, attributing changes to primary physiological effects at the level of each individual organism in terms of fatty acid (or molecular species) content alone seems rather uncertain. The change in lipid composition would appear here to be more closely tied to overall changes in community structure because we investigated a complex biofilm. Fatty acids alone may not provide sufficient information as they could, masking weaker effects like photoperiod

duration in favor of other environmental factors (i.e. simultaneous contamination exposure). Therefore, our suggestion is that some molecular species, especially those from PCs and DGDGs here (Table 2), may be more specific markers of light duration at a biofilm scale. In addition, the literature remains sparse at this level of molecular information, and we suggested to use similar lipidomic approach with monospecific cultures of microalgal strains to strengthen our preliminary results.

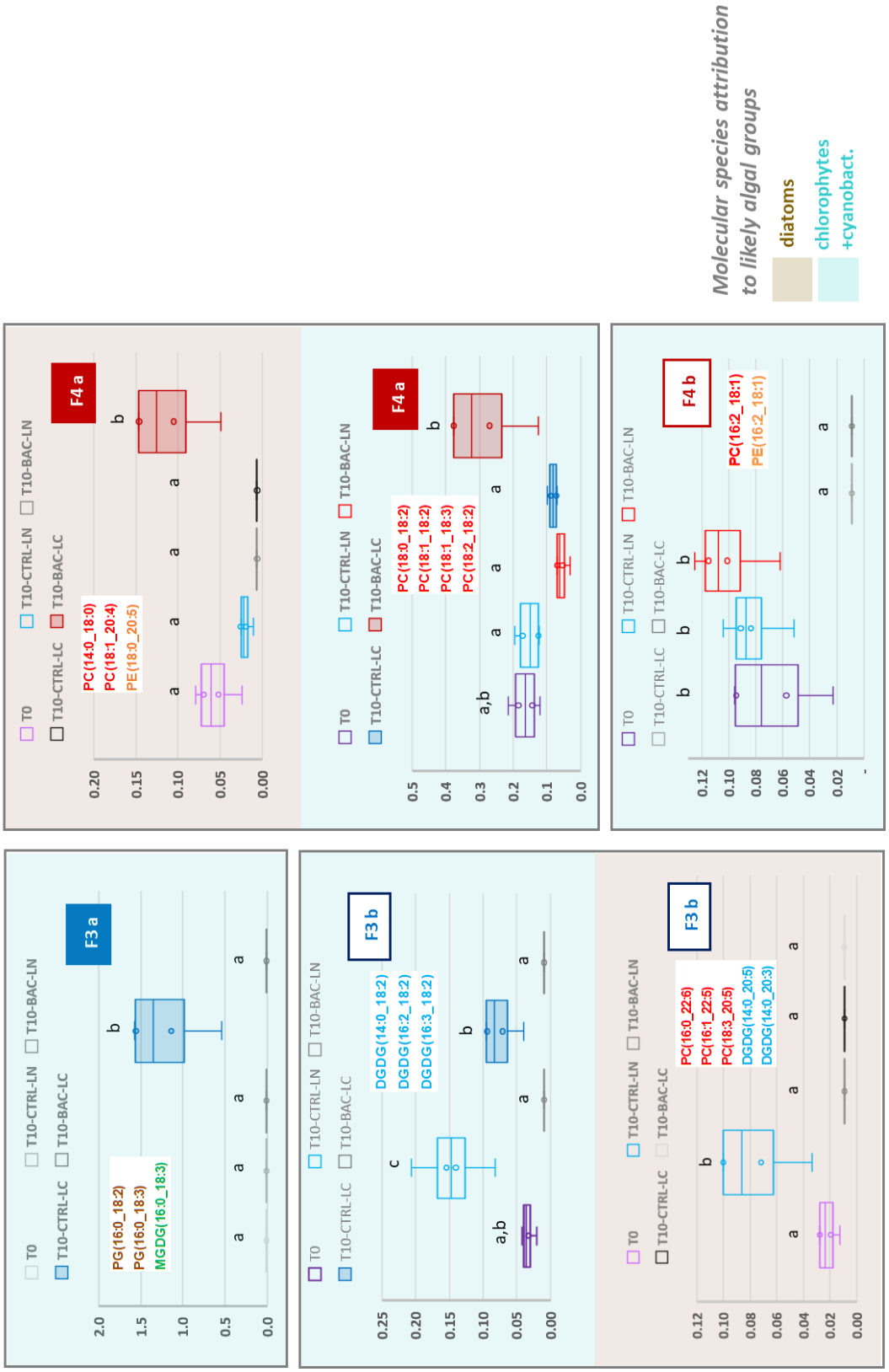

505

506 Figure 9. Variation of molecular species (nmol mg^{-1}) clusters selected for each group of
507 variables (F3 a and b, F4 a and b) as a function of time (T0 or T10), BAC 12contamination
508 (CTRL or BAC) and light condition (CL or NL). The distinction was also made based on the
509 probable origin of the molecular species, according to the known and representative fatty acids
510 of certain photoautotroph groups.

Conclusions

After exposing biofilm to BAC 12, the fatty acid deduced from polar lipid analysis suggested that the heterotrophic compartment would likely increase at the expense of phototrophic organisms. The overall reduction in PUFAs found on the same samples points to a sharp decline in all phototrophic organisms present in the biofilm. To more clearly separate the co-occurring effects of biocide exposure and light condition at the algal group level, the molecular species compositions of MGDG, DGDG, PG, PE, and PC were examined. The most representative molecular species were clustered, and it was proposed that certain molecular species, particularly those from PCs and DGDGs, could potentially act as more accurate markers of light duration at the biofilm scale. To strengthen our early results, it would be beneficial to use a similar lipidomic approach with monospecific cultures of microalgal strains, since the literature is still lacking at this level of both molecular in-depth details and understanding of the physiological mechanisms.

Author contributions

Nicolas MAZZELLA: Lipid analysis, Data analysis, Writing - original draft, review & editing.

Romain VRBA: Conceptualization, Investigation, Methodology, Sample preparation

Aurélie MOREIRA: Lipid and micropollutant analyses

Nicolas CREUSOT: Writing - review & editing.

Mélissa EON: Sample preparation, Physico-chemical analysis

Débora MILLAN-NAVARRO: Physico-chemical and micropollutant analyses

Isabelle LAVOIE: Funding acquisition, Supervision, Writing - review & editing.

Soizic MORIN: Funding acquisition, Supervision, Conceptualization, Writing - review & editing.

Conflicts of interest

None

Acknowledgements

The authors would like to acknowledge the financial support from the Institut National de Recherche pour l'Agriculture, l'alimentation et l'Environnement (INRAE) and l'Institut National de la Recherche, Scientifique (INRS).

References

Arts, M. T., R. G. Ackman, and B. J. Holub. 2001. Essential fatty acids in aquatic ecosystems: a crucial link between diet and human health and evolution. Can J Fish Aquat Sci **58**:122−137.

Bergé, J.-P., J.-P. Gouygou, J.-P. Dubacq, and P. Durand. 1995. Reassessment of lipid composition of the diatom, Skeletonema costatum. Phytochemistry **39**:1017-1021.

Bhatia, I. S., R. K. Raheja, and D. S. Chahal. 1972. Fungal lipids. I. Effect of different nitrogen sources on the chemical composition. Journal of the Science of Food and Agriculture **23**:1197-1205.

Brown, M. R., G. A. Dunstan, S. J. Norwood, and K. A. Miller. 1996. Effects of harvest stage and light on the biochemical composition of the diatom *Thalassiosira pseudonana*. Journal of Phycology **32**:64-73.

Chaumet, B., S. Morin, O. Hourtané, J. Artigas, B. Delest, M. Eon, and N. Mazzella. 2019. Flow conditions influence diuron toxicokinetics and toxicodynamics in freshwater biofilms. Science of The Total Environment **652**:1242-1251.

Coniglio, D., M. Bianco, G. Ventura, C. D. Calvano, I. Losito, and T. R. I. Cataldi. 2021. Lipidomics of the Edible Brown Alga Wakame (Undaria pinnatifida) by Liquid Chromatography Coupled to Electrospray Ionization and Tandem Mass Spectrometry. Molecules **26**:4480.

Dalsgaard, J., M. St. John, G. Kattner, D. Müller-Navarra, and W. Hagen. 2003. Fatty acid trophic markers in the pelagic marine environment. Pages 225-340 Advances in Marine Biology. Academic Press.

Demailly, F., I. Elfeky, L. Malbezin, M. Le Guédard, M. Eon, J.-J. Bessoule, A. Feurtet-Mazel, F. Delmas, N. Mazzella, P. Gonzalez, and S. Morin. 2019. Impact of diuron and S-metolachlor on the freshwater diatom Gomphonema gracile: Complementarity between fatty acid profiles and different kinds of ecotoxicological impact-endpoints. Science of The Total Environment **688**:960-969.

Doumenq, P., M. Acquaviva, L. Asia, J. P. Durbec, Y. Le Dréau, G. Mille, and J. C. Bertrand. 1999. Changes in fatty acids of Pseudomonas nautica, a marine denitrifying bacterium, in response to n-eicosane as carbon source and various culture conditions. FEMS Microbiology Ecology **28**:151-161.

Dunstan, G. A., J. K. Volkman, S. M. Barrett, J.-M. Leroi, and S. W. Jeffrey. 1993. Essential polyunsaturated fatty acids from 14 species of diatom (Bacillariophyceae). Phytochemistry **35**:155-161.

Fadhlaoui, M., V. Laderriere, I. Lavoie, and C. Fortin. 2020. Influence of Temperature and Nickel on Algal Biofilm Fatty Acid Composition. Environmental Toxicology and Chemistry **39**:1566-1577.

Filimonova, V., F. Gonçalves, J. C. Marques, M. De Troch, and A. M. M. Gonçalves. 2016. Fatty acid profiling as bioindicator of chemical stress in marine organisms: A review. Ecological Indicators **67**:657-672.

Fuschino, J. R., I. A. Guschina, G. Dobson, N. D. Yan, J. L. Harwood, and M. T. Arts. 2011. Rising water temperatures alter lipid dynamics and reduce n-3 essential fatty acid concentrations in scenedesmus obliquus (Chlorophyta). J Phycol **47**:763-774.

Goss, R., and T. Jakob. 2010. Regulation and function of xanthophyll cycle-dependent photoprotection in algae. Photosynth Res **106**:103–122.

Guschina, I. A., and J. L. Harwood. 2006. Lipids and lipid metabolism in eukaryotic algae. Progress in Lipid Research **45**:160-186.

Guschina, I. A., and J. L. Harwood. 2009. Algal lipids and effect of the environment on their biochemistry. Springer New York.

Lang, I., L. Hodac, T. Friedl, and I. Feussner. 2011. Fatty acid profiles and their distribution patterns in microalgae: a comprehensive analysis of more than 2000 strains from the SAG culture collection. BMC plant biology **11**:124-124.

Li-Beisson, Y., J. J. Thelen, E. Fedosejevs, and J. L. Harwood. 2019. The lipid biochemistry of eukaryotic algae. Progress in Lipid Research **74**:31-68.

Mazzella, N., M. Fadhlaoui, A. Moreira, and S. Morin. 2023a. Molecular species composition of polar lipids from two microalgae Nitzschia palea and Scenedesmus costatus using HPLC-ESI-MS/MS. ChemRxiv.

Mazzella, N., J. Molinet, A. D. Syakti, J.-C. Bertrand, and P. Doumenq. 2007. Assessment of the effects of hydrocarbon contamination on the sedimentary bacterial communities and determination of the polar lipid fraction purity: Relevance of intact phospholipid analysis. Marine Chemistry **103**:304-317.

Mazzella, N., J. Molinet, A. D. Syakti, A. Dodi, J.-C. Bertrand, and P. Doumenq. 2005. Use of electrospray ionization mass spectrometry for profiling of crude oil effects on the phospholipid molecular species of two marine bacteria. Rapid Communications in Mass Spectrometry **19**:3579-3588.

Mazzella, N., A. Moreira, M. Eon, A. Médina, D. Millan-Navarro, and N. Creusot. 2023b. Hydrophilic interaction liquid chromatography coupled with tandem mass spectrometry method for quantification of five phospholipid classes in various matrices. MethodsX **10**:102026.

Napolitano, G. E. 1999. Fatty Acids as Trophic and Chemical Markers in Freshwater Ecosystems. Pages 21-44 *in* M. T. Arts and B. C. Wainman, editors. Lipids in Freshwater Ecosystems. Springer New York, New York, NY.

Opute, F. I. 1974. Lipid and Fatty-acid Composition of Diatoms. Journal of Experimental Botany **25**:823-835.

Robert, S., M. Mansour, and S. Blackburn. 2007. Metolachlor-Mediated Selection of a Microalgal Strain Producing Novel Polyunsaturated Fatty Acids. Marine biotechnology (New York, N.Y.) **9**:146-153.

Sakagami, Y., H. Yokoyama, H. Nishimura, Y. Ose, and T. Tashima. 1989. Mechanism of resistance to benzalkonium chloride by Pseudomonas aeruginosa. Applied and Environmental Microbiology **55**.

Sohlenkamp, C., and O. Geiger. 2015. Bacterial membrane lipids: diversity in structures and pathways. FEMS Microbiology Reviews **40**:133-159.

Vestal, J. R., and D. C. White. 1989. Lipid Analysis in Microbial Ecology: Quantitative approaches to the study of microbial communities. BioScience **39**:535-541.

Vrba, R., I. Lavoie, N. Creusot, M. Eon, D. Millan-Navarro, A. Feurtet-Mazel, N. Mazzella, A. Moreira, D. Planas, and S. Morin. 2023. Impacts of urban stressors on freshwater biofilms. bioRxiv:2023.2006.2011.544504.

Wacker, A., M. Piepho, and E. Spijkerman. 2015. Photosynthetic and fatty acid acclimation of four phytoplankton species in response to light intensity and phosphorus availability. European Journal of Phycology **50**:288-300.

Wada, H., and N. Murata. 1998. Membrane Lipids in Cyanobacteria. Pages 65-81 *in* S. Paul-André and M. Norio, editors. Lipids in Photosynthesis: Structure, Function and Genetics. Springer Netherlands, Dordrecht.

Wang, B., and J. Jia. 2020. Photoprotection mechanisms of Nannochloropsis oceanica in response to light stress. Algal Research **46**:101784.

Zäuner, S., W. Jochum, T. Bigorowski, and C. Benning. 2012. A cytochrome b5-containing plastid-located fatty acid desaturase from Chlamydomonas reinhardtii. Eukaryot Cell **11**:856-863.

Zelles, L. 1997. Phospholipid fatty acid profiles in selected members of soil microbial communities. Chemosphere **35**:275-294.

Zulu, N. N., K. Zienkiewicz, K. Vollheyde, and I. Feussner. 2018. Current trends to comprehend lipid metabolism in diatoms. Progress in Lipid Research **70**:1-16.

647

Appendices

Table A 1. BAC 12 concentrations (mg L^{-1}) in the four experimental conditions at T10. BAC 12 = contaminated biofilm; CTRL = non-exposed biofilm; NL = alternated photoperiod; CL = Continuous photoperiod.

Conditions	BAC 12 concentrations
T10-CTRL-NL	< 0.01
T10-BAC-NL	27.03 ± 12.12
T10-CTRL-CL	< 0.01
T10-BAC 12-CL	17.20 ± 7.47

Table A 2. Mass spectrometry parameters (single ion monitoring) for free fatty acid analysis.

Fatty acid	Q1 (m/z)	dwell time (ms)	DP (V)	CE (V)
C14:0	243	30	70	20
C15:0	257	30	70	20
C16:4	263	30	70	20
C16:3	265	30	70	20
C16:2	267	30	70	20
C16:1	269	30	70	20
C16:0	271	30	70	20
C17:1	283	30	70	20
C17:0	285	30	70	20
C18:4	291	30	70	20
C18:3	293	30	70	20
C18:2	295	30	70	20
C18:1	297	30	70	20
C18:0	299	30	70	20
C19:0	313	30	70	20

C20:5	317	30	70	20
C20:4	319	30	70	20
C20:1	325	30	70	20
C20:0	327	30	70	20
C22:6	343	30	70	20
C22:5	345	30	70	20

Table A 3. Chromatographic analytical gradient for free fatty acids separation.

Time (min)	**% of A** (5 mM ammonium acetate)	**% of B** (acetronitrile:isopropanol, 50:50)	**Flow rate (µL min^{-1})**
0	50	50	300
0.3	50	50	300
5.8	1	99	300
8.8	1	99	300
9.1	50	50	300
11	50	50	300

663 Table A 4. Polar lipid-derived and free fatty acids data.

Polar + free FA	T0				T10-CTRL-NL				T10-BAC-NL			
C (nmol/mg)	rep1	rep2	rep3	rep4	rep1	rep2	rep3	rep4	rep1	rep2	rep3	rep4
C14:0	0.5	0.9	2.9	1.1	1.7	1.2	1.3	0.9	0.4	0.1	0.1	0.1
C16:3	1.6	0.9	1.4	1.2	0.8	1.3	0.4	1.1	-	-	-	-
C16:2	2.3	1.6	3.1	3.1	0.2	0.6	0.6	0.2	0.4	0.4	0.6	0.4
C16:1	15.9	3.2	9.5	15.8	4.2	1.7	11.8	6.0	9.7	4.9	8.7	8.2
C16:0	4.6	1.9	10.0	3.2	7.2	6.8	5.6	1.1	13.1	4.6	6.2	2.1
C18:3	0.6	0.3	1.0	0.9	1.7	1.4	0.8	0.5	-	-	-	-
C18:2	1.1	1.4	1.4	0.4	1.0	1.2	1.0	1.4	0.1	0.1	0.2	0.1
C18:1	2.7	2.1	0.9	3.5	2.3	2.2	2.6	2.5	0.7	0.6	4.6	9.2
C18:0	0.1	0.1	0.1	0.3	0.0	0.1	0.2	0.2	0.2	0.2	0.2	0.2
C20:5	1.2	6.2	1.9	3.8	1.1	1.8	3.3	4.0	-	-	-	-
C20:4	0.9	0.4	0.3	0.2	0.0	0.2	0.2	0.1	-	-	-	-
C20:3	0.1	0.0	0.1	0.1	0.0	0.0	0.0	0.0	-	-	-	-
C20:2	0.4	0.2	0.3	0.3	0.2	0.1	0.1	0.1	-	-	-	-
C20:0	1.6	1.0	2.2	0.9	0.3	0.3	0.1	0.2	-	-	-	-
C22:6	0.7	0.8	0.8	0.8	0.4	0.1	0.1	0.4	-	-	-	-
C22:5	0.0	-	-	0.1	-	0.0	0.0	0.0	-	-	-	-
Sum (nmol/mg)	34.0	20.8	35.9	35.6	21.0	18.9	28.2	18.5	24.5	10.8	20.6	20.2

SFAs (%)	20%	18%	42%	15%	44%	44%	26%	13%	56%	44%	32%	11%
MUFAs (%)	55%	25%	29%	54%	31%	21%	51%	46%	42%	51%	65%	86%
PUFAs (%)	26%	56%	28%	30%	26%	35%	23%	41%	2%	5%	4%	2%
PUFA/(SFA+MUFA) (%)	0.34	1.29	0.40	0.43	0.34	0.54	0.30	0.70	0.02	0.05	0.04	0.02
UFA/SFA (%)	4.04	4.44	1.36	5.51	1.29	1.25	2.91	6.62	0.80	1.25	2.17	7.76
BAFA (%)	21%	19%	31%	20%	45%	48%	30%	21%	57%	50%	54%	57%

Polar + free FA	T10-CTRL-CL				T10-BAC-CL			
C (nmol/mg)	rep1	rep2	rep3	rep4	rep1	rep2	rep3	rep4
C14:0	1.3	0.7	0.9	0.9	0.1	0.2	0.1	0.1
C16:3	0.4	0.8	0.4	0.4	-	-	-	-
C16:2	0.8	0.7	0.5	0.3	0.5	0.5	0.2	0.6
C16:1	7.0	4.9	7.7	5.1	4.4	10.8	4.6	5.1
C16:0	6.1	4.8	3.2	5.6	7.6	1.4	3.0	9.8
C18:3	1.1	1.4	1.8	1.3	0.0	0.0	0.0	0.0
C18:2	1.3	0.4	1.3	0.0	0.6	0.5	0.2	0.5
C18:1	2.3	0.2	0.5	2.0	3.0	3.4	3.9	5.8
C18:0	0.1	0.1	0.1	0.1	0.2	0.1	0.1	0.0
C20:5	5.8	4.1	3.8	4.6	0.1	0.2	0.2	0.1
C20:4	0.3	0.3	0.3	0.3	0.0	0.0	0.0	0.0
C20:3	-	-	-	-	-	-	-	-
C20:2	0.2	0.1	0.2	0.0	-	-	-	-
C20:0	0.2	0.9	0.3	0.8	-	-	-	-
C22:6	-	0.5	0.2	0.4	-	-	-	-
C22:5	0.0	0.0	0.0	0.0	-	-	-	-
Sum (nmol/mg)	26.8	20.0	21.1	21.8	16.6	17.1	12.4	22.1

SFAs (%)	29%	32%	21%	34%	47%	10%	26%	45%
MUFAs (%)	35%	25%	39%	33%	45%	83%	68%	49%
PUFAs (%)	37%	42%	40%	34%	8%	7%	6%	6%
PUFA/(SFA+MUFA) (%)	0.58	0.73	0.67	0.50	0.08	0.07	0.06	0.06
UFA/SFA (%)	2.51	2.09	3.71	1.95	1.11	8.77	2.86	1.22
BAFA (%)	32%	26%	18%	35%	65%	29%	57%	71%

664

665

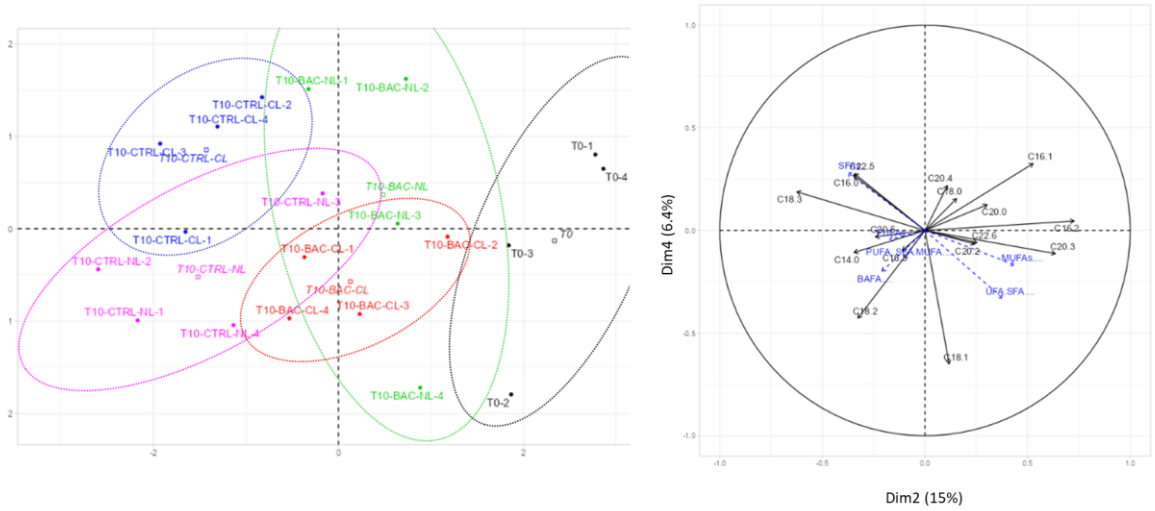

666

667 Figure A 1. Dimensions 2 and 4 of the PCA for fatty acids.

668

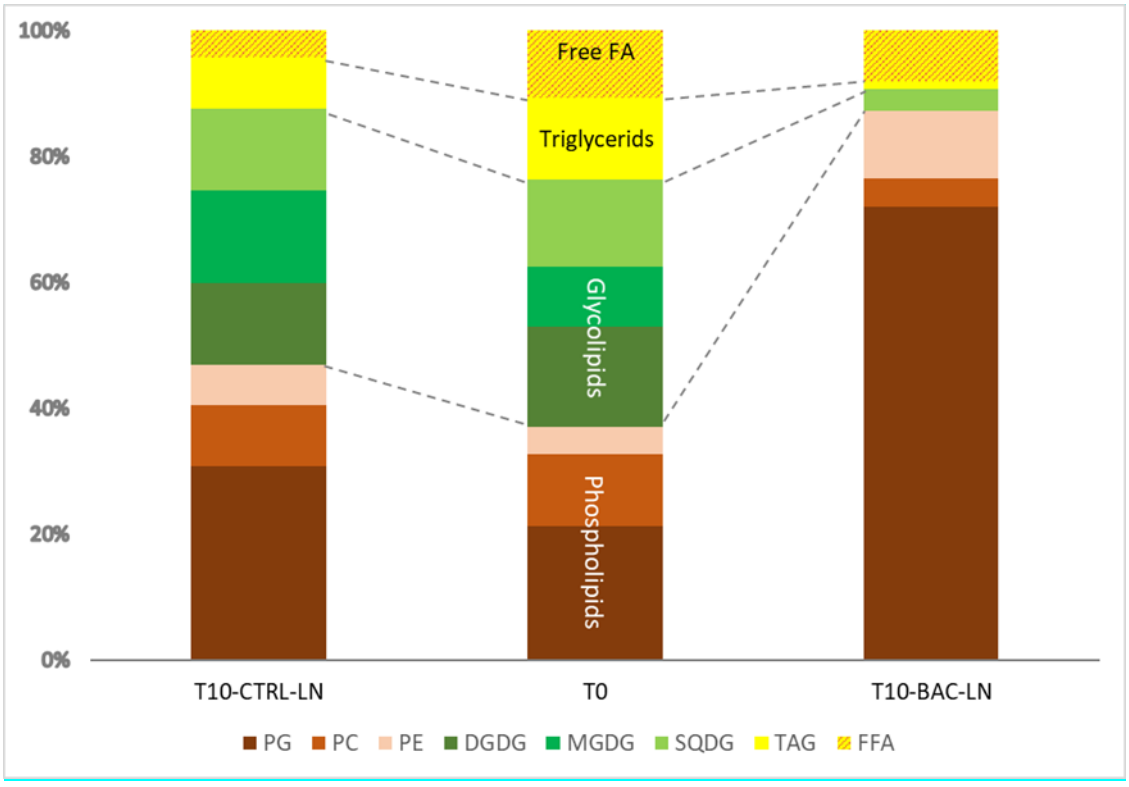

669

670 Figure A 2. Average lipid classes and FFA relative proportions.

671

672

673

674 Table A 5. Fatty acids as variables filtered by cos^2 values.

Polar lipid FA	Cos^2>0.5 (F1+F2)
C20:0	**0.881**
C16:3	**0.875**
C16:2	**0.867**
C22:6	**0.807**
C20:5	**0.761**
C22:5	**0.752**
C20:4	**0.728**
C20:3	**0.727**
C18:3	0.615
C18:1	0.552
C20:2	0.545
C16:1	0.545
C18:0	0.522

675

676

677

678

679

680 Table A 6. Multivariate analysis of variance for both PUFA/(MUFA+SFA) and GL/PL ratios.

MANOVA

MANOVA: Pillai Test ▼

Cases	df	Approx. F	$Trace_{Pillai}$	Num df	Den df	p
(Intercept)	1	32.123	0.889	2	8.000	1.504×10^{-4}
Light	1	0.977	0.196	2	8.000	0.417
BAC12 (mg L-1)	1	14.321	0.782	2	8.000	0.002
Light ✳ BAC12 (mg L-1)	1	3.904	0.494	2	8.000	0.066
Residuals	9					

681

682

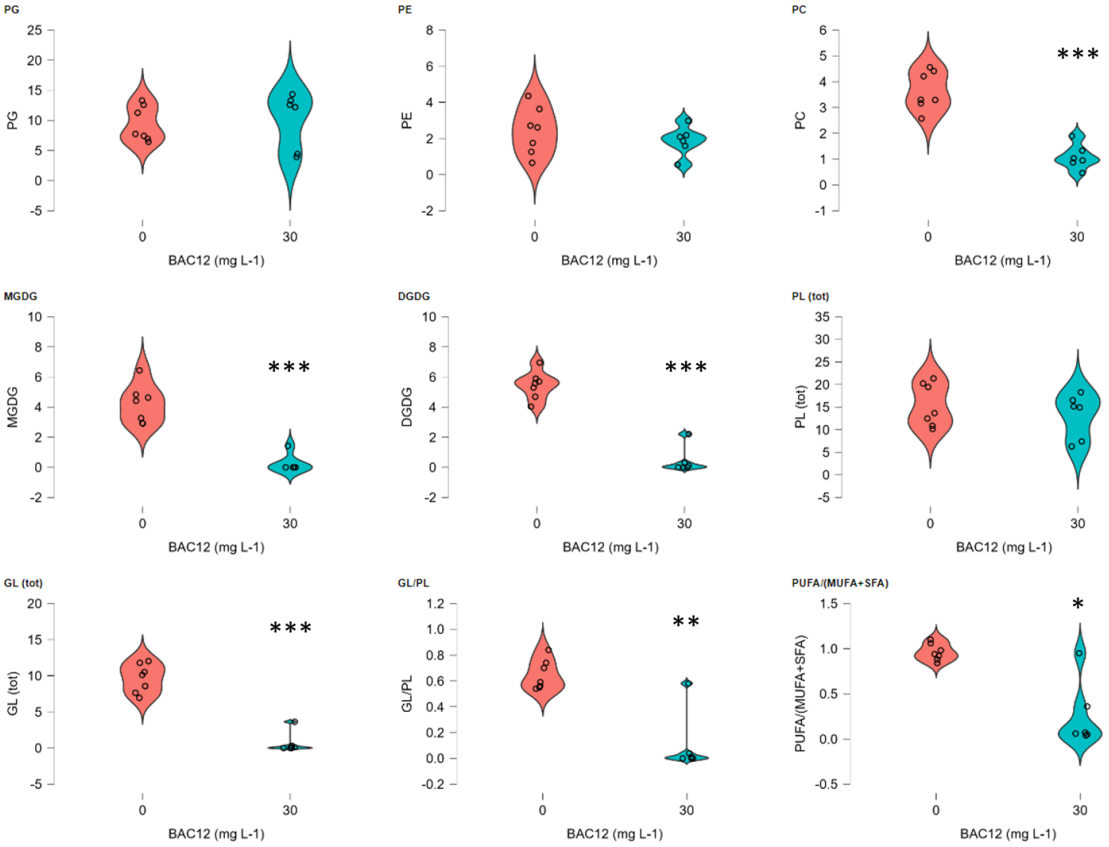

683

684 Figure A 3. Univariate (Welch's ANOVA) representation for each polar lipid class as well as
685 PUFA/(MUFA+SFA) and GL/PL ratios according to BAC 12 exposure. * for p<0.05, ** for p<0.01,
686 *** for p<0.001.

687

688

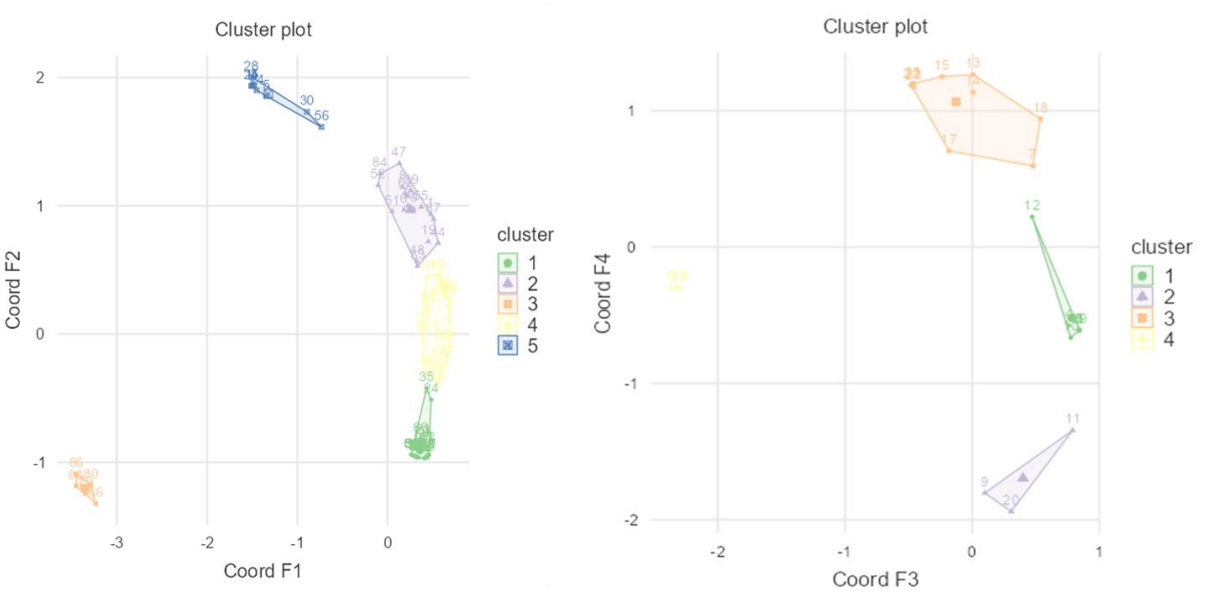

689

690 Figure A 4. k-means clustering of variables best represented in either F1-F2 or F3-F4 plans.

691

692

693